Available online at www.sciencedirect.com

ScienceDirect

www.elsevier.com/locate/jmbbm

Research paper

Morphological and mechanical characterization of composite bone cement containing polymethylmethacrylate matrix functionalized with trimethoxysilyl and bioactive glass

Mervi Puska[a,b,*], *Niko Moritz*[a], *Allan J. Aho*[a], *Pekka K. Vallittu*[a,c]

[a]*Institute of Dentistry, Department of Biomaterials Science and Turku Clinical Biomaterials Centre (TCBC) and BioCity Turku Biomaterials Research Program, Itäinen Pitkäkatu 4 B, 20520 Turku, Finland*
[b]*Nordic Institute of Dental Materials–NIOM, University of Oslo, Oslo, Norway*
[c]*Welfare Division, Turku, Finland*

ARTICLE INFO

Article history:
Received 25 September 2015
Received in revised form
10 December 2015
Accepted 14 December 2015
Available online 21 December 2015

Keywords:
Acrylic bone cement
Hybrid matrix polymer
Porosity
Bioactive composite
Micro-CT

ABSTRACT

Medical polymers of biostable nature (*e.g.* polymethylmetacrylate, PMMA) are widely used in various clinical applications. In this study, novel PMMA-based composite bone cement was prepared. Bioactive glass (BAG) particulate filler (30 wt%) was added to enhance potentially the integration of bone to the cement. The polymer matrix was functionalized with trimethoxysilyl to achieve an interfacial bond between the matrix and the fillers of BAG. The amount of trimethoxysilyl in the monomer system varied from 0 to 75 wt%. The effects of dry and wet (simulated body fluid, SBF at +37 °C for 5 weeks) conditions were investigated. In total, 20 groups of specimens were prepared. The specimens were subjected to a destructive mechanical test in compression. Scanning electron microscopy (SEM) and micro-computed tomography (micro-CT) were used to study the surface and the three-dimensional morphology of the specimens. The results of the study indicated that the addition of trimethoxysilyl groups led to the formation of a hybrid polymer matrix which, in lower amounts (<10 wt% of total weight), did not significantly affect the compression properties. However, when the specimens stored in dry and wet conditions were compared, the water sorption increased the compression strength (~5–10 MPa per test group). At the same time, the water sorption also caused an evident porous structure formation for the specimens containing BAG and siloxane formation in the hybrid polymer matrix.

*Corresponding author at: Turku Clinical Biomaterial Centre (TCBC), Itäinen Pitkäkatu 4 B, Fl-20520 Turku, Finland. Tel.: +358 2 333 8388; fax: +358 2 333 8390.
E-mail address: mervi.puska@utu.fi (M. Puska).

http://dx.doi.org/10.1016/j.jmbbm.2015.12.016
1751-6161/

1. Introduction

Polymethylmethacrylate (PMMA) or related polymers are used as bone cements or synthetic bone substitutes in various clinical applications. Despite their widespread use in the knee and hip replacements since the 1970s (Charnley, 1960; Lewis, 1997; Mousa et al., 1999), the main limitation of the family of acrylic bone cements is their relatively low bioactivity, exothermic polymerization reaction, toxicity of monomers and brittleness of the polymer. Shortly (~7–10 min) before the implantation, the powder and liquid components of acrylic bone cements are mixed together, which leads to a radical polymerization reaction of liquid acrylic monomers, *i.e.* methylmethacrylate (MMA) or related monomers (Revell et al., 1998). In fact, the use of acrylic bone cements has been criticized, primary, due to the lack of proper adherence between the bone cement and the surrounding bone. In conventional acrylic bone cements, the dense, non-porous structure of the material prevents bone ingrowth into the cement layer causing only mechanical fixation. Therefore, the regeneration of bone is limited to the interface between the bone cement and the bone. In mechanical fixation, the micromotion at the interface between bone and bone cement can lead to resorption of bone, and in the case of total hip replacements, possible loosening of the prosthesis (Santavirta et al., 1998). In addition, the following shortcomings of acrylic bone cements have been reported: low mechanical properties compared to cortical bone, chemical necrosis of bone due to the release of unreacted monomers and volume shrinkage during the polymerization (Revell et al., 1998; Lewis, 1997; Ciapetti et al., 2000; Gilbert et al., 2000). There are several possibilities to avoid these problems, *e.g.* by altering of the mixing methods, by adding of bioactive and reinforcing components or by developing the radiopaque agent system (Mousa et al., 1999; Lewis, 2000; Puska et al., 2003, 2004; Lewis, 2006).

Like most biological materials, bone is a composite like material, where particulate, porous, and fibrous structures are present (Kazt, 1996). Likewise, in acrylic bone cements, the addition of filler particles in matrix change the original properties *e.g.* increase the stiffness, improve the creep resistance or fracture toughness (Gasser, 2000). Therefore, the final properties of a composite are a result of interaction between the properties of every constituent phase, *i.e.* (a) the matrix, (b) filling components, and (c) the interfacial region between the filling components and the matrix polymer (Hull and Clyne, 2002). In the case of different modifications of bone cements, the aim is adjust their properties closer to those of bone. In fact, the first porous acrylic bone cement was already developed in the middle of the 1970's. In those studies, a porous PMMA was formed by the incorporation of a dispersing agent into the acrylic bone cement (Rijke et al., 1977; Bruens et al., 2003). Later, the group of Prof. Rui L. Reis performed similar studies, in which the corn starch/cellulose acetate (with or without hydroxyapatite) was incorporated into an acrylic bone cement system (Boesel et al., 2004; Espigares et al., 2002). According to the *in vivo* studies, porous PMMA-based bone cements offered a scaffold structure suitable for bone ingrowth (Rijke et al., 1977; Bruens et al., 2003; Puska et al., 2006).

Our studies are focused on the modification of biostable bone cements in order to improve their biological properties, for example, by creating porosity and bioactive structure in the cement matrix (Puska et al., 2009). Basically, bioactive materials (*e.g.* bioactive glass, BAG) have a functionally reactive surface which promotes the formation of a bond between the tissue and the material (Hench and Paschall, 1973; Hench, 1973; Vallittu et al., 2015). In particulate composites, the lack of proper bonding between the filler particles and the matrix often results in poor mechanical properties. Therefore, when BAG filler is added to acrylic polymer matrix, the interfacial properties of these two types of materials should be adjusted using a coupling agent. Typically, silanes are applied as synthetic hybrid organic–inorganic compounds across glass particulate or fiber surfaces and acrylic polymer matrix (Puska et al., 2009; Oral et al., 2014). The usefulness of silanes relies on their molecular structure. However, if bioactive glass particles are silanized, there is a risk that the outermost reactive surface will be covered by silane layer and the bioactivity of BAG will be inhibited. In this study, a survey was done to find out whether the presence of 3-methacryloxypropyltrimethoxysilane (MPS) (Fig. 1) as a co-monomer in a two-liquid monomer system of acrylic bone cement increases the adhesion between BAG and matrix polymer of acrylic bone cement. In addition, the test

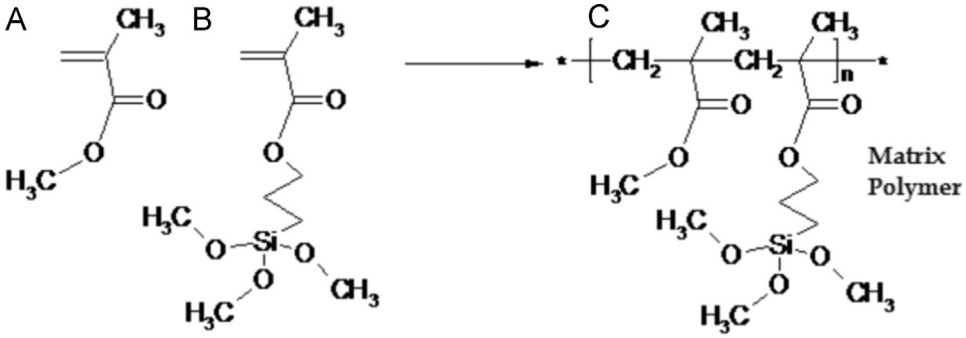

Fig. 1 – The curing of experimental acrylic bone cement composites was based on the free radical polymerization of vinyl monomers, *i.e.* methylmethacrylate (MMA, A) and 3-methacryloxy-propyltrimethoxysilane, (®MPS, B). The formed matrices (C) in groups 1–10 were contained an altering amount of trimethoxysilyl groups, randomly distributed, depending on the amount of MPS in the monomer system.

specimens of this study were also subjected to wet conditions, *i.e.* soaking in SBF for 5 weeks.

2. Materials and methods

2.1. Acrylic bone cement

Table 1 shows the chemical ingredients of the cement as reported by the manufacturer. Each dose of autopolymerizing Palacos® bone cement consisted of a powder component (40 g), where the main ingredient was a poly(methylacrylate, methyl methacrylate), PMMA–PMA, copolymer, and a liquid component (18.0 g) of MMA monomer as a main ingredient.

2.2. Simulated body fluid (SBF)

Table 2 shows the composition of Kokubo's SBF (Cho et al., 1995). SBF was prepared by dissolving reagent chemicals of NaCl, $NaHCO_3$, KCl, $K_2HPO_4 \times 3H_2O$; $MgCl_2 \times 6H_2O$, $CaCl_2 \times 2H_2O$; and Na_2SO_4 in deionized and distilled water (Milli-RO Plus 30 de-ionized water, with a resistivity of 18 MΩ cm, Millipore). The fluid was buffered at physiological pH 7.40, at 37 °C with tris(hydroxymethyl)aminomethane (50 mM) and hydrochloric acid (HCl).

Table 1 – Chemical composition of Palacos®R.

Powder	**40 g**
Poly(methylacrylate, methyl methacrylate), PMMA–PMA	33.8 g
Benzoyl peroxide	0.2 g
Zirconium dioxide	6.0 g
Chlorophyll (colorant E141)	0.001 g
Liquid	**18.8 g**
Methylmethacrylate (MMA) (stabilized with *ca.* 60 ppm hydroquinone)	18.4 g
N, N-Dimethyl-p-toluidine	0.4 g
Chlorophyll (colorant E141)	0.0004 g

Table 2 – The ion concentrations of SBF, pH 7.4 at 37 °C.

Ion	Concentration/mM
Na^+	142.0
K^+	5.0
Mg^{2+}	1.5
Ca^{2+}	2.5
Cl^-	147.8
HCO_3^-	4.2
HPO_4^{2-}	1.0
SO_4^{2-}	0.5

2.3. Preparation of the modified acrylic bone cement

Table 3 shows the materials used for the preparation of test specimens. Table 4 contains detailed information on the groups of the specimens. In polymer groups, the powder component of Palacos®R was used as such. In composite groups, the powder component also contained BAG granules (BonAlive™, S53P4, composition: SiO_2 53%, Na_2O 23%, CaO 20% and P_2O_5 4%, Ø315–505 μm, Vivoxid Ltd., Turku, Finland). The total amount of BAG was 30 wt%. A two-liquid monomer system, *i.e.* containing MMA and MPS (98%, Sigma-Aldrich Ltd., Steinheim, Germany), was mixed with the powder component for 5 min. In polymer groups and in composite groups, the monomer system contained 0, 12.5, 25, 37.5, 50, 62.5 or 75 wt% of MPS. Hence, the mixed test specimens paste contained totally 68 wt% of powder component and 32 wt% of monomer system. No additional initiator and activator of autopolymerisation reaction (based on the materials obtained from Palacos®R) were added in the preparation of test specimens. The prepared specimens were allowed to cure under normal temperature and pressure (NTP) conditions in the molds (cylindrical-shapes, diameter: 4.5 mm and height: 9 mm), thereafter they were divided in 20 groups ($N=6$/test group) according to the amount of MPS added and BAG (Table 4.). The polymer and composite specimens were subjected to two different storing conditions, *i.e.* dry and immersion in SBF at +37 °C for 5 weeks. During SBF-treatment, the test specimens were stored in a temperature-controlled water bath filled with a vibrator (Model Grant OLS-200, Cambridge, United Kingdom).

2.4. Compression properties

The compressive strength and the moduli of the specimens were measured according to the modified version of ISO 5833 (ISO5833/1:1979(E), 1979), using Lloyd's materials testing

Table 3 – The materials used in the study.

Brand	Manufacturer	Lot no.	Type of material
Palacos®R powder	Schering-Plough, Labo n.v. Heist-op-den-Berg, Belgium	8-BHAA-8/9033	Polymer
Palacos® liquid	Schering-Plough, Labo n.v. Heist-op-den-Berg, Belgium	8-RDCA-27/2969	Monomer
3-methacryloxy-propyltrimethoxy-silane, MPS	Sigma-Aldrich Ltd., Steinheim, Germany		Co-monomer
BAG, S53P4, BonAlive™	Vivoxid Ltd., Turku, Finland		Filler

Table 4 – Experimental groups of specimens, $N=8$ per group.

Material	Environmental conditions	Amount of MPS co-monomer of the total monomer content [wt%]							BAG content [wt%]
Polymer	dry	0	12.5	25.0	37.5	50	62.5	75	0
Composite	dry	0	12.5	25.0	37.5	50	62.5	75	30
Polymer	SBF	0	12.5	25.0	37.5	50	62.5	75	0
Composite	SBF	0	12.5	25.0	37.5	50	62.5	75	30

machine (Lloyds LR 30 K, Lloyds Instruments, United Kingdom). The compression force was applied along the axis the load speed of 1 mm/min. The compression strength was calculated from the load–deformation curve. The average compressive strength and standard deviation were calculated. The compression strength (CS) and the compression modulus (E) were calculated using the following formulae:

$$CS = F/A, \quad (1)$$

$$E = \Delta\delta/\Delta\epsilon, \quad (2)$$

where F is the applied load (N) at the highest point of the load–deflection curve, A is the area of the test specimen, $\Delta\delta$ is $\Delta F_i = A$, where F_i is the applied load (N) at the point i of the straight-line portion of the trace, $\Delta\varepsilon$ is $\Delta l_i/L$; where L is the length of the specimen, and l_i is the deflection corresponding to load F_i at a point in the straight-line portion of the trace. The data of compression strength and modulus were presented as the means and standard deviations (SD) of six repetitions.

2.5. Scanning electron microscopy

To determine the distribution of glass particles in the PMMA matrix and the formed porosity, the composite specimens were studied with SEM (Model JSM 35 CF, JEOL, Tokyo, Japan). The specimens were dried *ca*. 24 h in a desiccator before the analysis, and the surfaces were coated with a gold layer (thickness = 17 nm) using a sputter coater (Model BAL-TEC SCD 050 Sputter Coater, Balzers, Liechtenstein). The specimen surfaces were scanned with SEM at an accelerating voltage of 12 kV with different magnifications, and the outermost surface morphology of the specimens was analyzed (Fig. 2). To evaluate the pore dimensions, the SEM images were opened in an image-processing software. The apparent pores were manually outlined, excluding the pores extending beyond the image borders. For each outlined area, the average geometrical dimensions were assessed. Thereafter, a more detailed investigation was performed using micro-CT.

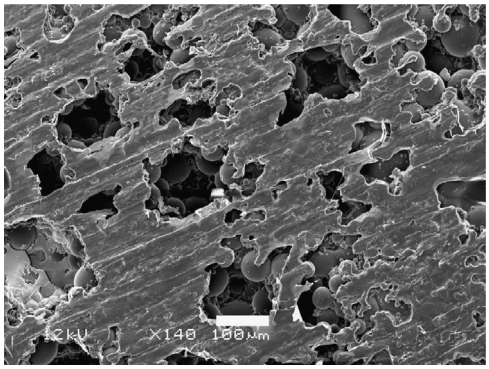

Fig. 2 – The outermost surface of a composite specimen contained 30 wt% of BAG particulate filler and 75 wt% of MPS as co-monomer after immersed in wet conditions for 5 weeks. The magnification is ×140, and the length of measuring rod 100 μm.

2.6. Micro-computed tomography

Micro-CT was used to study the three-dimensional structure of the specimens. Micro-CT imaging was performed with the spatial resolution of 5.23 μm/voxel. Source voltage was 72 kV and source current was 138 μA. Angular step was 0.45°, within the total angular range of 180°. At each angular step a shadow projection 16 bit image was taken. This image was an average of two consequent imaging. The shadow projection images were reconstructed into a stack of cross-sectional images using NRecon software (SkyScan, Belgium). A 4-mm thick cylindrical volume of interest (VOI) was selected within the stack of cross-sectional images and analyzed using CTAn software (SkyScan, Belgium).

2.7. Statistical analysis

Statistical analysis was performed using IBM SPSS Statistics software (Version 19, SPSS Inc., IBM Corp., USA). Kolmogorov–Smirnov test was used to verify the compliance of the data with the normal distribution. Data were analyzed with ANOVA, followed by Tukey posthoc analysis. The fixed factors were the amount of MPS co-monomer in the specimen and the environmental conditions (dry or SBF). The dependent variables were the compression strength and modulus. In addition, two-tailed Spearman correlation analysis was performed to study the relation of compression strength and modulus with the MPS content.

3. Results

3.1. Compression properties

Results of compression testing are shown in Figs. 3 and 4. In dry conditions, polymer specimens without MPS (0 wt% MPS) had mean compression strength of 58 MPa. The highest measured value was 71 MPa with 25 wt% MPS and the lowest was 27 MPa with 75 wt% MPS. Anova analysis revealed statistically significant increase in compression strength with the increase in MPS content up to 37.5 wt% of MPS. With 50 wt% of MTS, the compression strength was similar to that measured for polymer specimens without the addition of MPS (0 wt% MPS). With further increase in MPS content, the compression strength decreased and reached its minimum at 75 wt% MPS. Spearman correlation analysis performed for specimens with MPS content in the range of 0–37.5 wt% revealed a positive correlation with correlation coefficient $Rs = 0.349$ ($P = 0.04$), indicating a statistically significant improvement of compression strength in-line with the results Anova analysis. However, when all the data (0–75 wt% MPS) were analyzed, Spearman correlation indicated a decline in compression strength as a function of MPS content, $Rs = -0.498$ ($P < 0.01$).

For composite specimens measured in dry conditions, there was a statistically significant decline in compression strength as a function of MPS content indicated by Anova and Spearman correlation analysis, $Rs = -0.895$ ($P < 0.01$). The highest value was 70 MPa with 0% MPS and the lowest was 23 MPa with 75 wt% MPS.

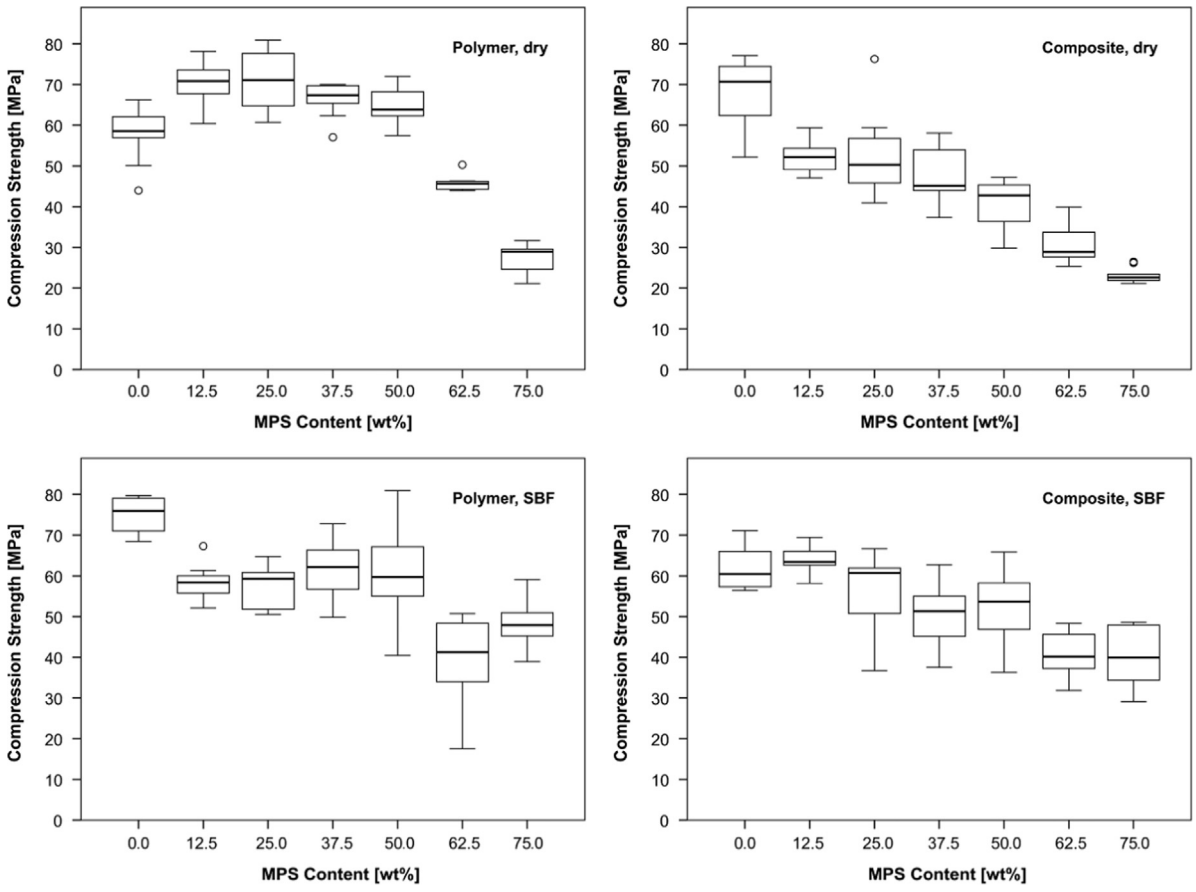

Fig. 3 – Compression strengths of the test specimens containing from 0 to 75 wt% of MPS as co-monomer. Polymer specimens contained no BAG particulate whereas composite specimens contained 30 wt% of BAG particulate filler. Prior to testing, polymer and composite specimens were either stored in dry conditions (dry) or were immersed in SBF for 5 weeks (SBF).

For polymer specimens measured after immersion in SBF, there was a statistically significant decrease in compression strength as a function of MPS content indicated by Anova and Spearman correlation analysis, $Rs = -0.470$ ($P < 0.01$). The highest value was 75 MPa with 0% MPS and the lowest was 48 MPa with 75 wt% MPS.

For polymer specimens measured after immersion in SBF, there was a statistically significant decrease in compression strength as a function of MPS content indicated by Spearman correlation analysis, $Rs = -0.313$ ($P = 0.012$). Anova indicated a statistically significant decline in compression strength in the range of 62.5–75 wt% MPS. The highest compression strength value was 64 MPa with 12.5% MPS and the lowest was 40 MPa with 75 wt% MPS.

Statistical analysis (Anova) was also done within each MPS content group. A comparison was made between polymer and composite specimens in dry conditions and after immersion in SBF. For dry specimens, the addition of BAG significantly affected the compression strengths of the specimens in the range of MPS content from 0 to 62.5 wt%. However, without MPS (0 wt%), composite specimens had statistically higher compression strength compared with polymer specimens. In all other MPS content groups composite specimens were inferior to polymer specimens. For polymer and composite specimens tested after immersion in SBF, there were no statistically significant differences in the value of compression strength in the whole range of MPS content (0–75 wt%).

SBF treatment had a statistically significant effect on polymer specimens. For specimens without MPS (0 wt% MPS), there was an increase in compression strength. For specimens with 12.5 and 25 wt% MPS, the specimens immersed in SBF were inferior to dry specimens. For specimens with 75 wt% MPS, SBF treatment fairly improved the compression strength. For composite specimens with high content of MPS (50–75 wt%), SBF treatment led to statistically significant differences in compression strength, with dry specimens being superior.

MPS content had a marginal effect on compression modulus. Only dry polymer specimens exhibited a correlation between the MPS content and the compression modulus. In the in the range of 0–37.5 wt% MPS, there was a positive correlation, $Rs = 0.463$ ($P < 0.01$). In the whole MPS range, 0–75 wt%, there was a negative correlation. Anova indicated a statistically significant increase in compression modulus was found between specimens without MPS (0 wt% MPS) and specimens with 37.5 wt% MPS. In addition, there was a statistically significant decrease in compression modulus between specimens without MPS (0 wt% MPS) and specimens with 75 wt% MPS.

For dry composites, as well as polymers and composites immersed in SBF, there were no statistically significant

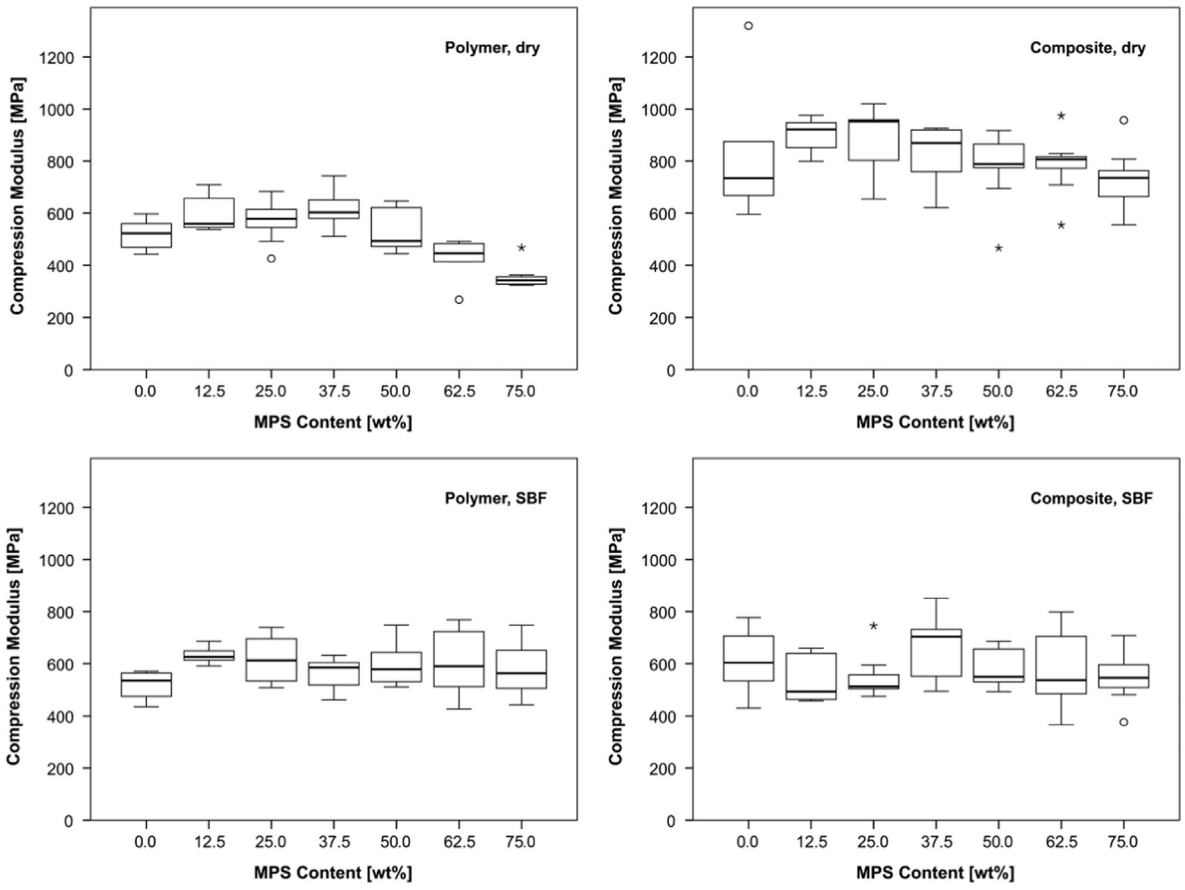

Fig. 4 – Compression modulus of the test specimens containing from 0 to 75 wt% of MPS as co-monomer. Polymer specimens contained no BAG particulate whereas composite specimens contained 30 wt% of BAG particulate filler. Prior to testing, polymer and composite specimens were either stored in dry conditions (dry) or were immersed in SBF for 5 weeks (SBF).

correlations between MPS content and compression modulus. Anova revealed no statistically significant differences.

Statistical analysis (Anova) was also done within each MPS content group. For dry specimens, the addition of BAG significantly increased the compression modulus of the specimens in the whole range of MPS content from 0 to 75 wt%. However, for SBF-treated specimens there was no statistically significant effect of the addition of BAG.

Statistically significant effect of SBF treatment on polymer specimens was observed for specimens with high content of MPS (62.5–75 wt%). In contrast there was a statistically significant negative effect of the SBF-treatment on composite specimens in the range of 12.5–75 wt% MPS.

3.2. *Scanning electron microscopy (SEM) analysis*

Fig. 2 shows a SEM micrograph of the outermost surface of a composite specimen contained 30 wt% of BAG particulate and 75 wt% of MPS as co-monomer after immersed in wet conditions for 5 weeks. The average size of the pores on the surface was in a scale of 10–200 μm, though abundant large pore-sizes (~200–500 μm) were also observed.

3.3. *Micro-CT analysis*

According to the results micro-CT image analysis, water sorption caused a porous structure formation for the composite specimens with 30 wt% BAG and hybrid polymer matrix. In the quantitative porosity analysis, the pores (Fig. 5) were homogenously distributed. Figs. 6 and 7 show the distribution of pore-sizes and wall thickness. The main distribution of pore-sizes were *ca.* 20–60 μm (>85 vol%), whereas there were also a considerable amount of large pore-sizes (50–130 μm). The total porosity indicated by micro-CT analysis was 17.7%, of which open porosity (interconnected pores) was 10.5%.

4. Discussion

The synthetic bone substitutes (including acrylic bone cements) have traditionally been in the form of granules, gel, injectable/putty-like cements. However when compared with auto- and allografts, these synthetic biomaterials do not always have adequate biological acceptance Therefore, there is a constant need to search for better synthetic bone substitute materials. Adjustable porosity, bioactivity and adequate biomechanics, are central for achieving a durable bone-bonding (Aho et al., 2004). If the bonding is not good

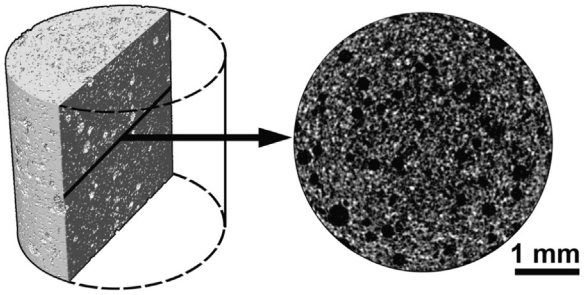

Fig. 5 – Composite specimen, a three-dimensional surface rendering of the volume of interest, VOI (on the left), a cross-sectional image of the material, gray color represents polymer matrix and black color represents pores (on the right).

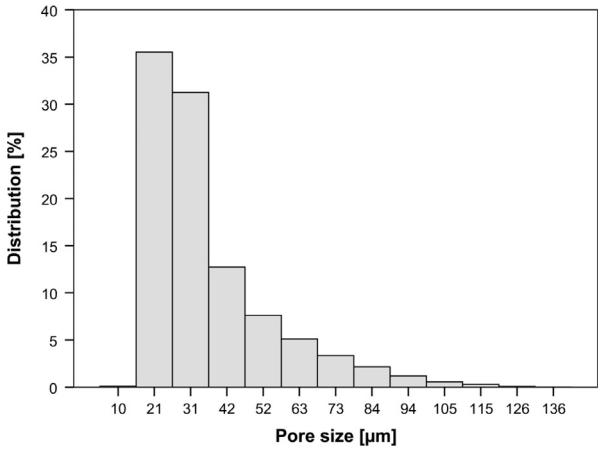

Fig. 6 – Pore-size distribution, the major distribution of pore-sizes was between 20 and 42 μm but also contained a significant amount of pores of 52–126 μm.

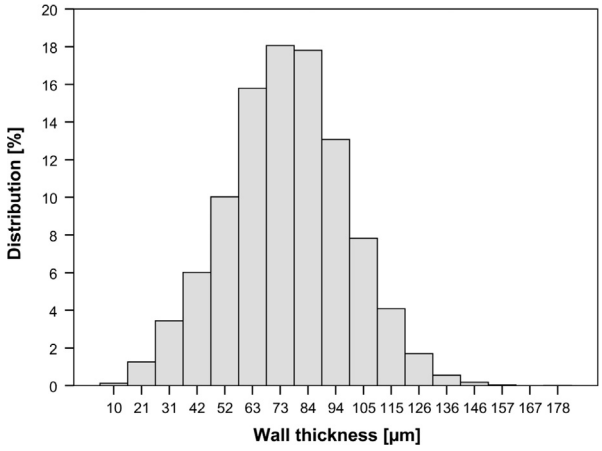

Fig. 7 – Distribution of wall thicknesses, the main distribution were between 60 and 90 μm (>50 vol%).

enough, the bone and cement interface is prone to micromotion, which can lead to the resorption of bone and release of material debris (Santavirta et al., 1998).

Synthetic bone substitutes can be divided into basic categories: (1) calcium phosphate (CaP) or calcium sulfate ($CaSO_4$) based materials, (2) BAGs and (3) polymers (*e.g.* PMMA) and their composites. The bone substitutes in categories (1) and (2) allow bioactive fixation (Hench and Paschall, 1973; Hench, 1973; Kenny and Buggy, 2003). However, these materials are brittle and thus not suitable for load-bearing applications. On the other hand, conventional bone cements do not allow bioactive fixation in host bone, although their biomechanics are suitable for cortical bone reconstruction (Lewis, 2006; Kenny and Buggy, 2003). Therefore, if bone ingrowth and bioactive fixation are needed, tailor-made composite structures can provide the solution. In these structures, the matrix polymer can be chosen from the category (3), and the bioactivity and porous structure can be achieved by using filler particulate, *e.g.* from categories (1) and (2).

Our earlier studies were focused on polyamide of hydroxyl-L-proline based pore-generating filler modified acrylic bone cement. The reduced mechanical properties of porous structures could be offset by using fiber-reinforcement and a semi-interpenetrating network, semi-IPN (Puska et al., 2003, 2004, 2009, 2004). Moreover, acrylic bone cements containing bioactive glass (~60–70 wt%) have been reported to have a significantly higher bone-bonding strength than plain PMMA cement (Mousa et al., 1999; Ohtsuki et al., 2006; Mori et al., 2005; Tsukeoka et al., 2006; Kamimura et al., 2002). In addition, Miyazaki et al. (2003) have suggested that the apatite formation, prerequisite for bone-bonding, could be induced by a silanol (Si–OH) group, originated from MPS co-monomer and formed in the hybrid matrix, as well as by the dissolution of calcium ion (Ca^{2+}) from the material (Miyazaki et al., 2003).

In terms of polymer matrix in this study, for specimens stored in dry conditions, the 25% MPS concentration increased strength and modulus, which was not found after storing in wet conditions. This could be related to the formation of silane originated inorganic phase, which reinforces the material, but which is prone for hydrolysis. This interesting finding indicates that the formed polymer matrix was an organic–inorganic hybrid. However, contrary to our expectations, for specimens stored in dry conditions the addition of BAG into hybrid matrix decreased the compression strength regardless of the MPS content. This finding suggests that there was an inadequate adhesion between trimethoxysilyl groups and the hydroxyl groups of BAG. Therefore, the tensile and shear stresses present during the compression test were present at the weak interface of the filler and the matrix leading to the fracture propagation. As expected, the formed porosity also caused the decrease in the compression strength. The porosity increases the heterogeneity of the bone cement leading to the decrease in the mechanical properties. Thus, in the porous structures, the energy needed for crack propagation is much lower than in dense structures. Apparently, to achieve the reinforcing effect between trimehoxysilyl or siloxane groups and particles of BAG, the amount of MPS should be lower, *i.e.* <10 wt% in monomer system, and the loading of particles of BAG should be evaluated thoroughly.

In a composite, the polymer–inorganic interface is normally formed within the polymer, and failures often occur within the polymer or at the interface (Karacaer et al., 2001). Hence, it is the matrix polymer together with the interface chemistry that mainly controls the adhesion. Therefore, the interface of filler and matrix should be adjusted either (a) by

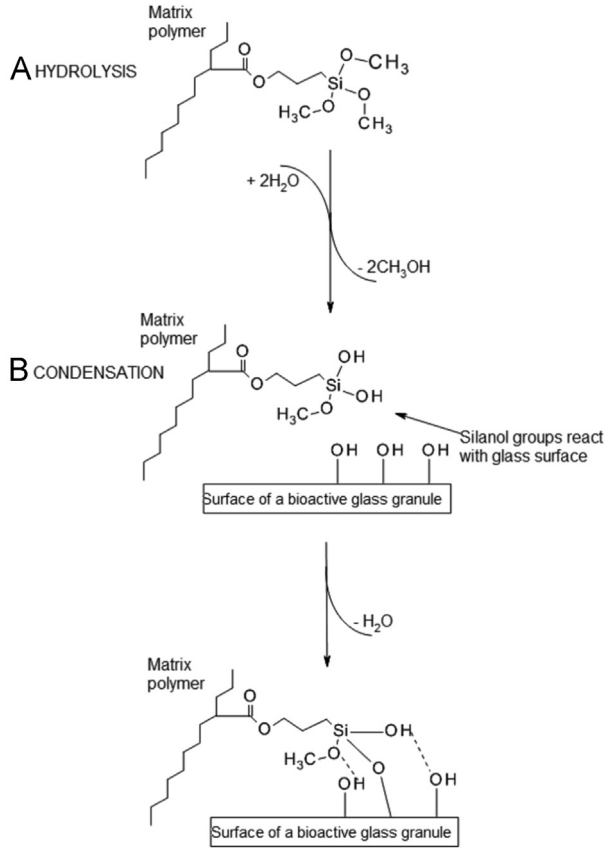

Fig. 8 – In the hydrolysis (A), trimethoxysilyl groups of matrix polymer are activated by the diffusion of water molecules. In the condensation reaction, the activated silanols are able to react with the hydroxyl groups, thus bridging the matrix to the surface of bioactive glass granules. In the adhesion interface, there are possible to be covalent bonds as well as hydrogen bonds and ionic interaction.

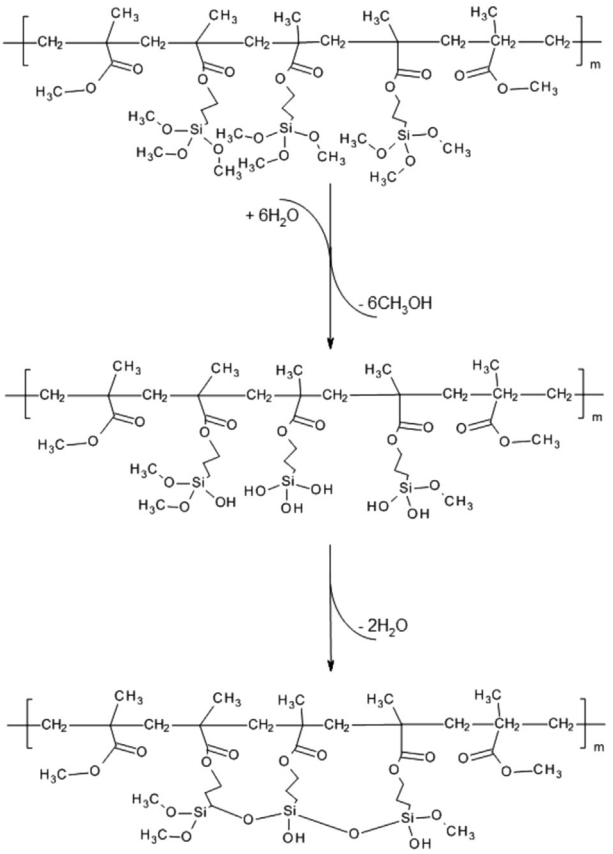

Fig. 9 – As simplified, in the hybrid matrix polymer, the presence of water molecules can cause intra-connected siloxane network formation. The first step forms silanol groups that can then react further with the other silanol groups existing in the same polymer chain or in the neighboring chain. In the matrix polymer, the silica gel or siloxane layer will then be obtained, while the existing hydroxyl groups are able to have interaction to the glass surface.

surface treatment or (b) by chemical grafting (Pape and Plueddemann, 1991; Zhang et al., 2000). Basically, silanes are used as adhesion promoters between silicon dioxide and matrix polymer (Puska et al., 2009). In this study, the new interesting information on the adhesion promotion of BAG particulate as well as porosity formation was obtained.

Fig. 8 shows a simplified presentation of the adhesion system between hybrid matrix polymer and glass surface that was intended in this study. In the hydrolysis step, the silanol groups are obtained by allowing the free trimethoxysilyl groups of matrix polymer to react with water molecules. After hydrolysis, a siloxane layer can be formed in the matrix or the silanol groups can further react with the hydroxyl groups on the glass. If the siloxane layer is formed in the matrix polymer, it consists of covalently and hydrogen-bonded organic molecules with acrylate functionality. Typically, if silane molecules are used for adhesion between matrix polymer and glass particles, they are activated by hydrolyzing the methoxy groups to become silanol groups at pH 5–6.5, *i.e.* in acidic conditions (Puska et al., 2009). Therefore, the test specimens of this study were also subjected to wet conditions, but at pH of body fluid. SBF was used as surrogate for extra cellular fluid. According to these results, the water sorption revealed that the diffusion of water most likely caused the hydrolysis reaction of silane groups that further led to reaction or interaction with the hydroxyl groups on the surface of BAG particles (Figs. 8 and 9).

In bone substitutes, the pore size should be large enough (100–500 μm) to allow vascularization and bone ingrowth (Galante et al., 1971; Moore et al., 2004). Although the optimal pore size is still under debate, considerably smaller pore sizes were suggested to allow bone ingrowth (Bobyn et al., 1980; Lu et al., 1999; Itälä et al., 2001). In this study, according to the analysis of SEM and micro-CT images (Figs. 2 and 5), an evident porosity has formed. In fact, the porous phase is not easily formed into the acrylic bone cement *in situ*. In most cases, the inert polymer matrix covers the outermost layer of well-embedded filler particles, thus hindering the porosity formation, *e.g.* when inorganic bioactive filler or pore-generating filler are used (Puska et al., 2003, 2009). The pore sizes of the studied specimens varied between 10 and 500 μm, were randomly distributed but formed an interconnected

network. Most likely, the porous structure has formed during the intra-condensation reaction of the silanol groups in the matrix polymer (Fig. 9). When the quantity of trimethoxysilyl groups increased, then the amount of pores also seemed to increase. Water is known to have a plasticizing effect on the hybrid polymer matrix cement. Therefore, water can easily penetrate into the matrix containing hydrophilic trimethoxysilyl groups, increasing the porosity of the matrix. This phenomenon was the most apparent in the case of composite structures. In fact, the glass surfaces increase the hydrophilic interfaces that facilitate water molecules diffusion easily through the whole material. The most effective water diffusion caused the hydrolysis reaction of trimethoxysilyl groups that most obviously continued the intra-condensation of silanol groups leading to the formation of the interconnected porosity. The intra-condensation between the silanol groups in the same polymer chain and/or to neighboring chains crosslinks the structure by either –O– bridges or OH–bonds, which also leads to the formation of porosity by the shrinkage of the structure and leaching of the components (*e.g.* methanol). At higher pH (7.4), the equilibrium of reaction is most likely due to the hydrolysis/intra-condensation of matrix, whereas the condensation to the glass surface does not occur as effectively as it would be in acidic conditions (Puska et al., 2009). Therefore, the adhesion layer between matrix polymer and glass surfaces is mainly based on the hydrogen bonds. Althought, the silanol groups from the glass surface are also able to interact with unhydrolysed trimethoxysilyl of matrix and form tightly bonded phases. Basically, the silanol groups have very strong polar interactivity and are responsible for the strong polar character. Therefore, hydrated silanol groups, on the phase of either matrix or glass, form a layer of polar components and water molecules in the interfaces of composites. In summary, in the groups with the high MPS content the compression strength was somewhat higher for SBF-treated composite specimens compared with the dry composite specimens possibly due to the interfacial interaction of hydrogen bonds were between matrix polymer and glass surfaces.

The addition of MPS co-monomer and 30 wt% of BAG-fillers adversely affected the working properties of cement. Namely, the composite became more viscous and more difficult to handle. In contrast, the working time became longer, and the composites were less sticky. In fact, the presence of BAG fillers might disturb the free radical polymerization. Therefore, in the coming studies, the reaction kinetics, like setting time, exothermal properties and the optimization of the powder/liquid component ratio, should be investigated in detail, as well as the optimal quantity of BAG. Moreover, the detailed information on the polymerization needs to be obtained by measuring the content of residual monomers as well as the degree of conversion of the acrylate groups. The amount of methanol, formed in the hydrolysis step, was not measured in this study. In the coming *in vivo* studies, the trimethoxy groups will be replaced by triethoxy groups in order to avoid the presence of methanol molecules. In addition, the reinforcing effect on mechanical properties will be studied using hyperbranched monomers, such as bifunctional or dendritic acrylate monomers. In fact, the addition of bifunctional monomer, like ethylene glycol dimethacrylate (EGDMA), has shown to reduce the quantity of released monomers and increase the mechanical properties (Puska et al., 2005).

However, one of the main limitations of the concept of the use of silanes within acrylic bone cements containing BAG particulate is related to the reactivity of the glass. When in contact with physiological fluids, the glass starts leaching the ions. This results in significant increase in local pH level in the proximity of the glass surface. In addition, the formation of the silica-rich layer on the surface of the glass leads to the precipitation of CaP which allows bone-bonding. There is a possibility that either the use of silanes may inhibit CaP precipitation, or the increase in local pH may disrupt the reactions occurring during silanization process. In fact both negative effects may occur.

5. Conclusions

The addition of MPS as co-monomer in acrylic bone cement increased the capability to absorb water that simultaneously ensured the increased adhesion between BAG and matrix polymer. In wet conditions, the modification of acrylic bone cement also caused the porosity formation and indicated bioactivity.

Acknowledgments

The authors gratefully acknowledge the Academy of Finland for funding (Grant no.: 128636, Biomimetic Self-assembling Bioadhesive (BASB) and 256337, Structure of Gradient Nanocomposites: Interaction of Bioactive Glasses with Nanoparticles and Polymers (MoreBAGS)). Also, the research has been partly funded by the Finnish Dental Society Apollonia. Study belongs to the BioCity Turku Biomaterials Research Program (www.biomaterials.utu.fi).

REFERENCES

Aho, A.J., Tirri, T., Kukkonen, J., Strandberg, N., Rich, J., Seppälä, J., Yli-Urpo, A., 2004. Injectable bioactive glass/biodegradable polymer composite for bone and cartilage reconstruction: concept and experimental outcome with thermoplastic composites of poly(epsilon-caprolactone-co-D,L-lactide) and bioactive glass S53P4. J. Mater. Sci.: Mater. Med. 15 (10), 1165–1173.

Bruens, M.L., Pieterman, H., de Wijn, J.R., Vaandrager, J.M., 2003. Porous polymethylmethacrylate as bone substitute in the craniofacial area. J. Craniofac. Surg. 14 (1), 63–68.

Boesel, L.F., Mano, J.F., Reis, R.L., 2004. Optimization of the formulation and mechanical properties of starch based partially degradable bone cements. J. Mater. Sci.: Mater. Med. 15 (1), 73–83.

Bobyn, J.D., Pilliar, R.M., Cameron, H.U., 1980. Weatherly GC. The optimum pore size for the fixation of porous-surfaced metal implants by the ingrowth of bone. Clin. Orthop. 150, 263–270.

Charnley, J., 1960. Anchorage of femoral head prosthesis to the shaft of the femur. J. Bone Jt. Surg. Br. 42B, 28–30.

Ciapetti, G., Granchi, D., Cenni, E., Savarino, L., Cavedagna, D., Pizzoferrato, A., 2000. Cytotoxic effect of bone cements in HL-60 cells: distinction between apoptosis and necrosis. J. Biomed. Mater. Res. 52, 338–345.

Cho, S.B., Nakanishi, K., Kokubo, T., Soga, N., 1995. Dependence of apatite formation on silica gel on its structure: effect of heat treatment. J. Am. Ceram. Soc. 78, 1769–1774.
Espigares, I., Elvira, C., Mano, J.F., Vázquez, B., San, R.J., Reis, R.L., 2002. New partially degradable and bioactive acrylic bone cements based on starch blends and ceramic fillers. Biomaterials 23 (8), 1883–1895.
Gilbert, J.L., Hasenwinkel, J.M., Wixson, R.L., Lautenschlager, E.P.J., 2000. A theoretical and experimental analysis of polymerization shrinkage of bone cement: a potential major source of porosity. J. Biomed. Mater. Res. 52, 210–218.
Gasser, B., 2000. About composite materials and their use in bone surgery. Injury 31 (Suppl 4), S48–S53.
Galante, J., Rostoker, W., Lueck, R., Ray, R.D., 1971. Sintered fiber metal composites as a basis for attachment of implants to bone. J. Bone Jt. Surg. Am. 53 (1), 101–114.
Hull, D., Clyne, T. (Eds.), 2002. An Introduction to Composite Materials. Cambridge University Press, Cambridge.
Hench, L.L., Paschall, H.A., 1973. Direct chemical bond of bioactive glass–ceramic materials to bone and muscle. J. Biomed. Mater. Res. 7 (3), 25–42.
Hench, L.L., 1973. Ceramics, glasses, and composites in medicine. Med. Instrum. 7 (2), 136–144.
ISO5833/1:1979(E), 1979. Implants for Surgery—Acrylic Resin Cements—Part I: Orthopaedic Applications. International Organization for Standardization. Geneva, Switzerland.
Itälä, A.I., Ylänen, H.O., Ekholm, C., Karlsson, K.H., Aro, H.T., 2001. Pore diameter of more than 100 m is not requisite for bone ingrowth in rabbits. J. Biomed. Mater. Res. 58 (6), 679–683.
Kazt, J.L., 1996. In: Ratner, B.D., Hoffman, A.S., Schoen, F.J., Lemons, J.E. (Eds.), Biomaterials Science, An Introduction to Materials in Medicine. Academic Press, San Diego, pp. 335–346.
Kenny, S.M., Buggy, M., 2003. Bone cements and fillers: a review. J. Mater. Sci.: Mater. Med. 14 (11), 923–938.
Kamimura, M., Tamura, J., Shinzato, S., Kawanabe, K., Neo, M., Kokubo, T., Nakamura, T., 2002. Bone-bonding strength of two kinds of poly(methyl methacrylate)-based bioactive bonecement containing bioactive glass beads or glass-ceramic powder. Key Eng. Mater. 218–220, 369–372.
Karacaer, O., Dogan, O.M., Tincer, T., Dogan, A., 2001. Reinforcement of maxillary dentures with silane-treated ultra high modulus polyethylene fibers. J. Oral Sci. 43 (2), 103–107.
Lewis, J., 1997. Properties of acrylic bone cement: state of the art review. J. Biomed. Mater. Res. 38 (2), 155–182.
Lewis, G., 1997. Properties of acrylic bone cement: state of the art review. J. Biomed. Mater. Res. 38, 155–182.
Lewis, G., 2000. Relative roles of cement molecular weight and mixing method on the fatigue performance of acrylic bone cement: simplex P versus osteopal. J. Biomed. Mater. Res. 53, 119–130.
Lewis, G., 2006. Injectable bone cements for use in vertebroplasty and kyphoplasty: state-of-the-art review. J. Biomed. Mater. Res. B: Appl. Biomater. 76, 456–468.
Lu, J.X., Flautre, B., Anselme, K., Hardouin, P., Gallur, A., Descamps, M., Thierry, B., 1999. Role of interconnections in porous bioceramics on bone recolonization in vitro and invivo. J. Mater. Sci. Mater. Med. 10 (2), 111–120.
Mousa, W.F., Kobayashi, M., Kitamura, Y., Zeineldin, I.A., Nakamura, T., 1999. Effect of silane treatment and different resin compositions on biological properties of bioactive bone cement containing apatite-wollastonite glass ceramic powder. J. Biomed. Mater. Res. 47 (3), 336–344.
Mori, A., Ohtsuki, C., Miyazaki, T., Sugino, A., Tanihara, M., Kuramoto, K., Osaka, A., 2005. Synthesis of bioactive PMMA bone cement via modification with methacryloxypropyltrimethoxysilane and calcium acetate. J. Mater. Sci.: Mater. Med. 16 (8), 713–718.
Miyazaki, T., Ohtsuki, C., Kyomoto, M., Tanihara, M., Mori, A., Kuramoto, K., 2003. Bioactive PMMA bone cement preparedby modification with methacryloxypropyltrimethoxysilane andcalcium chloride. J. Biomed. Mater. Res. 67A (4), 1417–1423.
Moore, M.J., Jabbari, E., Ritman, E.L., Lu, L., Currier, B.L., Windebank, A.J., Yaszemski, M.J., 2004. Quantitative analysis of interconnectivity of porous biodegradable scaffolds with micro-computed tomography. J. Biomed. Mater. Res. 71A (2), 258–267.
Oral, O., Lassila, L.V.J., Kumbuloglu, O.G., Vallittu, P.K., 2014. Bioactive glass particulate filler composite: effect of coupling of fillers and filler loading on some physical properties. Dent. Mater. 30 (5), 570–577.
Ohtsuki, C., Miyazaki, T., Kamitakahara, M., Tanihara, M., 2006. Design of novel bioactive materials through organic modification of calcium silicate. J. Eur. Ceram. Soc. 27 (2–3), 1527–1533.
Puska, M.A., Kokkari, A.K., Närhi, T.O., Vallittu, P.K., 2003. Mechanical properties of oligomer modified acrylic bone cement. Biomaterials 24 (3), 417–425.
Puska, M.A., Närhi, T.O., Aho, A.J., Yli-Urpo, A., Vallittu, P.K., 2004. Flexural properties of crosslinked and oligomer-modified glass-fibre reinforced acrylic bone cement. J. Mater. Sci.: Mater. Med. 15 (9), 1037–1043.
Puska, M., Aho, A.J., Tirri, T., Yli-Urpo, A., Vaahtio, M., Vallittu, P. K., 2006. Glass fibre reinforced porous bone cement implanted in rat tibia or femur: histological and histomorphometric analysis. Key Eng. Mater. 309–311 (2), 809–812.
Puska, M., Korventausta, J., Garoushi, S., Seppälä, J., Vallittu, P.K., Aho, A.J., 2009. Preliminary *in vitro* biocompatibility of injectable calcium ceramic–polymer composite bone cement. Key Eng. Mater. 396–398, 273–276.
Puska, M., Lassila, L., Vallittu, P.K., Seppälä, J., Matinlinna, J., 2009. Evaluation of Bis-GMA/MMA resin adhesion to silica-coated and silanized titanium. J. Adhes. Sci. Technol. 23, 991–1006.
Puska, M.A., Lassila, L.V., Närhi, T.O., Yli-Urpo, A., Vallittu, P.K., 2004. Improvement of mechanical properties of oligomer-modified acrylic bone cement with glass fibers. Appl. Compos. Mater. 11 (1), 17–31.
Pape, P.G., Plueddemann, E.P., 1991. Methods for improving the performance of silane coupling agents. J. Adhes. Sci. Technol. 5 (10), 831–842.
Puska, M.A., Lassila, L.V., Aho, A.J., Yli-Urpo, A., Vallittu, P.K., Kangasniemi, I., 2005. Exothermal characteristics and release of residual monomers from fiber-reinforced oligomer-modified acrylic bone cement. J. Biomater. Appl. 20 (1), 51–64.
Revell, P.A., Braden, M., Freeman, M.A., 1998. Review of the biological response to a novel bone cement containing poly (ethyl methacrylate) and n-butyl methacrylate. Biomaterials 19, 1579–1586.
Rijke, A.M., Rieger, M.R., McLaughlin, R.E., McCoy, S., 1977. Porous acrylic cement. J. Biomed. Mater. Res. 11 (3), 373–394.
Santavirta, S., Xu, J.W., Hietanen, J., Ceponis, A., Sorsa, T., Kontio, R., Konttinen, Y.T., 1998. Activation of periprosthetic connective tissue in aseptic loosening of total hip replacements. Clin. Orthop. Relat. Res. 352, 16–24.
Tsukeoka, T., Suzuki, M., Ohtsuki, C., Sugino, A., Tsuneizumi, Y., Miyagi, J., Kuramoto, K., Moriya, H., 2006. Mechanical and histological evaluation of a PMMA-based bone cement modified with .gamma.-methacryloxypropyltrimethoxysilane and calcium acetate. Biomaterials 27 (21), 3897–3903.
Vallittu, P.K., Närhi, T.O., Hupa, L., 2015. Fiber glass–bioactive glass composite for bone replacing and bone anchoring implants. Review. Dent. Mater. 31 (4), 371–381.
Zhang, Y., Tan, K.L., Zhang, J., Cui, C.Q., Lim, T.B., Kang, E.T., 2000. Thermal graft copolymerization-induced adhesion improvement of a FR-4/PETG laminate. Int. J. Adhes. 20 (2), 165–171.